Bioinspired Artificial [FeFe]-Hydrogenase with a Synthetic H-Cluster

Cécilia Papini, Constanze Sommer, Ludovic Pecqueur, Debajyoti Pramanik, Souvik Roy, Edward J. Reijerse, Florian Wittkamp, Vincent Artero, Wolfgang Lubitz, Marc Fontecave

A bioinspired artificial [FeFe]-hydrogenase with a synthetic H-cluster

C. Papini[1], C. Sommer[2], L. Pecqueur[1], D. Pramanik[3], S. Roy[3], E. J. Reijerse[2], F. Wittkamp[4], V. Artero[3], W. Lubitz[2], M. Fontecave[1*]

[1] Laboratoire de Chimie des Processus Biologiques, Collège de France-CNRS-Sorbonne Université, UMR 8229, 11 Place Marcelin Berthelot, 75231 Paris Cedex 05, France

[2] Max Planck Institute for Chemical Energy Conversion, Stiftstr. 34-36, 45470 Mülheim an der Ruhr, Germany

[3] Université Grenoble Alpes, CNRS, CEA Fundamental Research Division, Laboratoire de Chimie et Biologie des Métaux, 17 rue des Martyrs, F-38054 Grenoble Cedex 9, France

[4] Inorganic Chemistry I, Ruhr-University Bochum, Universitätsstrasse 150, 44780 Bochum, Germany

*Corresponding author: **Marc Fontecave** (marc.fontecave@college-de-france.fr), phone number +33 1 44 27 13 60

Abstract

[FeFe]-hydrogenases are powerful hydrogen evolution biocatalysts due to the activity of their unique metallocofactor, the H-cluster, derived from the association of a [4Fe-4S] cluster and a [2Fe]-subcluster, containing 2 CO and 2 CN^- ligands as well as an aza-propanedithiolate (adt^{2-}) ligand bridging the two Fe atoms. Various analogs of the H-cluster have been assembled in the iron-sulfur protein HydF, containing a [4Fe-4S] cluster, by reaction with a series of synthetic di-iron complexes mimicking the [2Fe]-subcluster of hydrogenases. The mimics contain a mixture of CO and CN^- ligands and various dichalcogenide (S or Se) bridging ligands. The resulting hybrid proteins have been characterized and shown to behave as active artificial hydrogenases. Based on the present structure-activity relationship study, we report that the most active and stable artificial hydrogenase was obtained with the mimic containing a propane di-selenol bridging ligand. This opens the possibility to develop a class of hydrogen-evolving enzymes with a synthetic active site mimicking that of the natural hydrogenase.

Keywords: hydrogenase, iron-sulfur cluster, selenium, artificial enzyme, hydrogen production

Introduction

Renewable energy storage through water splitting into H_2 and O_2 relies on the availability of cheap, abundant and efficient catalysts. Hydrogenases are metalloenzymes, based on first row transition metals, nickel and/or iron, which catalyze proton reduction to H_2 (HER: hydrogen evolution reaction) with remarkably high catalytic rates close to the thermodynamic equilibrium and, as such, they are intensely studied.[1] Furthermore, they have been shown to behave as exquisite catalysts when adsorbed on carbon electrodes opening the way to the fabrication of efficient bioelectrodes.[2] However, their technological development in practical devices is limited by their fragility, of which the foremost is their oxygen sensitivity.

Therefore, alternatives such as H_2-evolving bioinspired catalysts and artificial hydrogenases are being explored in parallel. First, easily accessible synthetic diiron and Ni-based complexes mimicking the organometallic active sites of the two major classes of hydrogenases, the [FeFe]- and [NiFe]-hydrogenases, respectively, as well as bioinspired cobalt complexes, have shown interesting HER activity.[3–6] However, they still suffer from large overpotentials, low catalytic rates and they are generally insoluble in aqueous solutions and often unstable during catalysis. In particular, with a few exceptions[7,8], they lack the critical components of the second coordination sphere provided in nature by the peptide chain surrounding the active metal center.

These concerns have recently led to the emergence of attempts aiming at developing artificial hydrogenases.[3,9,10] Artificial enzymology currently enjoys increasing interest as a way to expand the repertoire of enzymes, via anchoring a synthetic molecular catalyst (here a biomimetic HER catalyst) into a protein host, not necessarily an enzyme, through covalent or non-covalent interactions.[9] This strategy combines attractive features of both molecular and enzymatic catalysis. The protein environment might provide the synthetic catalysts a new coordination sphere, favoring catalysis through increased water solubility, greater activity and selectivity as well as greater stability. By encapsulating the catalyst, the protein prevents it from deactivation via bimolecular processes. Furthermore, such hybrid systems may have, with respect to natural hydrogenases, the following specific benefits: (i) much easier preparation in larger scales; (ii) tunability not only by mutagenesis of the protein's

secondary coordination sphere but also by synthetic variations of the catalyst (ligand and metal). The most significant results paving the way towards efficient artificial hydrogenases have recently been reviewed.[9,10,11,12]

Here we explore a specific class of artificial hydrogenases based on synthetic diiron organometallic complexes which are close mimics of the [2Fe]-subcluster (named [$2Fe^{HydA}$] in the following) of the active site (H-cluster) of [FeFe]-hydrogenases (named HydA) (Figure 1A). Each Fe atom of [$2Fe^{HydA}$] has one CO and one CN^- ligand and is connected to the other through a bridging CO ligand. The coordination sphere is completed by a unique aza-propanedithiolate (adt^{2-}) ligand bridging the two Fe atoms and a cysteine ligand shared with an adjacent [4Fe-4S] cluster to form the H-cluster, a [6Fe] unit.[1] In general bioinspired synthetic diiron complexes contain various combinations of CN^- and CO ligands on each Fe atom as well as a dithiolate bridging ligand (or close variants) and some of them display significant catalytic proton reduction activity in organic solvent.[3] There are a few interesting examples of such synthetic complexes incorporated into peptides or proteins resulting in functional artificial hydrogenases.[9–11,13–15]

A highly relevant and unique hybrid system containing a [6Fe] cluster highly reminiscent of the H-cluster in the HydA active site has been prepared in our laboratory. As a preliminary study, we showed that the biomimetic compound $[Fe_2(pdt)(CO)_4(CN)_2]^{2-}$ (compound **2** in Scheme 1; pdt^{2-} = propanedithiolate) can be easily incorporated into the [4Fe-4S] protein HydF, serving as a host protein.[16,17] The reason of choosing HydF lies in its capacity to transiently bind, as a natural maturase essential for HydA activation, the diiron precursor of [$2Fe^{HydA}$].[18] The structure of the metallocluster within the resulting hybrid protein has been established to be a [6Fe] unit in which the diiron complex is attached to the [4Fe-4S] cluster via a cyanide bridge (Figure 1B). This is possible because the [4Fe-4S] cluster is well exposed at the surface of the protein and is chelated by only three cysteines and a labile glutamate (E305 in *Thermosipho melanesiensis* HydF, simply called HydF in the following) making one Fe accessible to exogenous ligands, as shown by X-ray crystallography.[17,19] Using HydF from *Thermotoga maritima* and *Thermosipho melanesiensis*, we previously found that the $[Fe_2(pdt)(CO)_4(CN)_2]^{2-}$/HydF hybrid (named **2**-HydF in the following) displayed hydrogenase activity based on a standard chemical assay using sodium dithionite as the source of electrons and methyl viologen as a redox mediator.[16,17]

This hybrid system thus provides an interesting platform for further improvement towards more efficient artificial hydrogenases via site-directed mutagenesis of the protein host and synthetic manipulation of the diiron subunit. Here we report our recent efforts to expand the repertoire of semisynthetic proteins based on HydF and synthetic diiron complexes and evaluate their hydrogenase activity.

Results

Screening diiron complexes with HydF

In the following we name the hybrid protein as **x**-HydF, in which **x** represents the synthetic diiron complex (Scheme 1) and HydF is the protein host, containing the [4Fe-4S] cluster. We have prepared the seven diiron complexes shown in Scheme 1 which all contain one or two CN^- ligands expected to be necessary for binding to the [4Fe-4S] cluster of HydF. We have purified HydF (from *T. melanesiensis*) in the apo dimeric form and introduced the [4Fe-4S] cluster in a second step chemically according to previously reported procedures.[17] After this step HydF preparations usually contain 3.5 ± 0.4 Fe and 3.6 ± 0.2 S per polypeptide chain. We then produced a series of seven **x**-HydF hybrids: HydF has been incubated with 1-3 equivalents of complex and then desalted to remove the excess of ligand. The incorporation of the complexes into the protein has been monitored by UV-Visible spectroscopy since these compounds display a specific absorption band at around 350 nm. As an illustration of the light absorption properties of the free complex, HydF and the hybrid, the case of **4**-HydF is shown in Figure 2A. The spectrum contains the contribution of complex **4**, at 350 nm, and that of the [4Fe-4S] cluster expected at 410 nm. The spectra obtained with the other hybrids are shown in Fig. S1. The amount of complex bound to the protein was in each case obtained from a standard Fe quantitation assay and the data, based on three independent measurements, are reported in Table 1. It appears that the diiron complex occupancy ranged from 40 % to 150 %, with 100 % corresponding to a 1:1 **x**:HydF monomer stoichiometry.

Subsequently, the hydrogen evolution activity was determined using 4 µM of **x**-HydF in the presence of 4 mM dithionite, as the reducing agent, 4 mM methyl viologen, as a redox mediator, in 100 mM potassium phosphate pH 6 under anaerobic conditions at room temperature. Hydrogen evolution and quantitation were monitored during reaction using a miniaturized Clark-type electrochemical H_2-microsensor after

calibration of the electrode. In the absence of methyl viologen we observed a dramatic decrease in H_2 production and in the absence of the hybrid protein no H_2 could be detected. The obtained turnover frequencies (TOF) are calculated from the amount of H_2 produced during the first 5 minutes of the assay, and time-dependent H_2 formation curves are shown in Figure 2 for **4**-HydF as well as in Figures S2 for the other hybrids. HydF containing only the [4Fe-4S] cluster and apoHydF displayed no H_2 evolution activity (Figure 2B). With the exception of **4**, the diiron complexes free in solution were inactive under the assay conditions. Similarly, no catalytic activity could be observed in the case of **3**-HydF and, more surprisingly, also in the case of **1**-HydF. While a TOF value of 0.05 min^{-1} was found for **2**-HydF, in agreement with previously reported values[17], a slightly larger activity was found with **5**-HydF (0.12 min^{-1}), **6**-HydF (0.1 min^{-1}) and **7**-HydF (0.07 min^{-1}). The most interesting hybrid was **4**-HydF which not only achieved a relatively larger TOF value (0.65 min^{-1}) but in addition was able to sustain H_2 production for 50 min (Figure S5), corresponding to 20 turnovers, while all other hybrids stopped functioning after a few minutes (Figure S2). The inset in Figure 2B reports the pH dependence of the activity of **4**-HydF, showing increased activity with decreasing pH, as expected.

Thus, introduction of two terminal Se atoms in the bridging ligand of the diiron complex enhanced both activity and stability of the hybrid proteins (compare **2**-HydF and **4**-HydF as well as **1**-HydF and **5**-HydF). In contrast, hybrid proteins obtained by reaction of **2** or **4** with a HydF protein reconstituted with a [4Fe-4Se] cluster were much less active than the corresponding **2**-HydF and **4**-HydF (Figure S3). Fe quantitation assays showed that HydF, reconstituted with a [4Fe-4Se] cluster, contained 6.0 ± 0.2 and 6.3 ± 0.1 Fe atoms per polypeptide chain after reaction with **2** and **4** respectively. Thus, the presence of Se atoms in the cubane cluster has no effect on the ability of HydF to bind biomimetic diiron complexes.

***4**-hybrids obtained using HydF variants and HydA*

Finally, a first attempt to use site-directed mutagenesis for modulating the activity of **4**-HydF was carried out. Three HydF variants, in which the glutamate ligand (E305) of the [4Fe-4S] cluster was changed to a histidine, a cysteine or an alanine, were used to generate hybrid proteins with **4**. Almost stoichiometric incorporation of **4** into

E305C, E305H and E305A versions of HydF was observed (Table 1). Proton reduction assays showed that the **4**-HydF E305H mutant displayed the same activity as **4**-HydF, while the two other mutants, **4**-HydF E305C and **4**-HydF E305A, displayed much lower activity (Table 1 and Figure S4).

Since **4**-HydF proved to be the best artificial hydrogenase of the series studied, here we compare it to a **4**-HydA hybrid, obtained by treatment of MeHydA, the hydrogenase from *Megasphaera elsdenii*, in the form lacking the [2Fe]-subcluster [$2Fe^{HydA}$], with complex **4**, following the procedure used for HydF. Such a **4**-HydA hybrid has been previously reported using HydA from *Chlamydomonas reinhardtii* or *Clostridium pasteurianum*.[20] As previously reported, various analogs of the H-cluster can indeed be assembled in HydAs via the reaction of the HydA form lacking the [$2Fe^{HydA}$] subcluster with a [$2Fe^{HydA}$] mimic of the type shown in Scheme 1.[20–23] We show here that **4** was able to bind also to MeHydA (Table 1) and that the resulting **4**-HydA hybrid, with a TOF of 0.24 min^{-1}, was less active than **4**-HydF (Figure 2B), by a factor of approximately 2 after correction taking into account the different [2Fe] contents in **4**-HydF and **4**-HydA.

*Characterizing the **4**-HydF hybrid*

Besides UV-visible spectroscopy (Figure 1A) and Fe quantitation, the correct assembly of a pure [6Fe] cluster in **4**-HydF was also confirmed by Fourier transform infrared (FTIR) and EPR spectroscopy and by the observation that apoHydF, lacking the [4Fe-4S] cluster, could not bind complex **4**. FTIR spectroscopy is a convenient method for characterizing metalloproteins such as hydrogenases containing CO and CN^- ligands. As shown in Figure 2C, the FTIR spectrum of **4**-HydF contained CN^--stretching bands between 2,100 and 2,000 cm^{-1} and CO-stretching bands in the 2000-1850 cm^{-1} range. In general, the bands are slightly narrower than the FTIR bands of the unbound complex in solution and show a different signal pattern. This indicates that, while it indeed binds to the [4Fe-4S] cluster, the [2Fe] complex is still largely solvent exposed. The CN^- stretches are less broad possibly because of conserved and positively charged amino acids in close proximity[17] interacting with the CN^- ligands and thus lowering the conformational freedom. FTIR spectra of **4**-HydF (E305H, E305A, E305C) mutants are also shown in Figure S6, demonstrating correct incorporation of **4** within HydF mutants, with only minor shifts of the peaks with respect to **4**-HydF.

Reduction of **4**-HydF with dithionite resulted in only minor blueshifts of 2-4 cm^{-1} for the CO ligands suggesting redox activity only at the [4Fe-4S] cluster (Figure S7). This is borne out by the UV-Visible spectra of **4**-HydF reduced with sodium dithionite: besides the absorption band of dithionite at 315 nm, Figure S8 showed a decrease of the absorption band at 410 nm, reflecting the reduction of the $[4Fe\text{-}4S]^{2+}$ cluster into $[4Fe\text{-}4S]^{+}$, while the absorption band at 350 nm characteristic of complex **4** was unaltered.

Similar observations were obtained for the FTIR spectra of the **2**-HydF hybrid previously reported (Figure 2C).[17] As shown in Figure 2C the signal pattern for CN^- and CO bands of **4**-HydF was redshifted by 3–8 cm^{-1} compared to **2**-HydF, reflecting the replacement of S by Se. This is in good agreement with the redshifts found for complex **5** incorporated into HydA from *Clostridium pasteurianum*[21] as compared to **1**-HydA as well as with the redshifts found for **4** in HydA from *Chlamydomonas reinhardtii* as compared to **2**-HydA.[20] This change can be explained by the donation from the Se lone pair to the Fe σ*-orbital that enhances π-back-donation from Fe to CO/CN^-. We did not obtain any evidence for spontaneous release of the complex from HydF during prolonged incubation in buffers, as monitored by FTIR spectroscopy.

The cw-EPR spectra of HydF, **4**-HydF and **2**-HydF after reduction with dithionite under anaerobic conditions are shown in Figure 2D. The spectra are typical of a reduced $[4Fe\text{-}4S]^{+}$ cluster with a spin ground state S=1/2. Compared to HydF, **4**-HydF and **2**-HydF show small g value differences (see Table S1), indicating an interaction of the [4Fe-4S] cluster with the added complex, as previously reported.[17]

Discussion

As mimics of $[2Fe^{HydA}]$, the [2Fe]-subcluster of [Fe-Fe]-hydrogenases, organometallic diiron complexes, with a mixture of CO and CN^- ligands and a dithiolate bridge, have been extensively studied as catalysts for photo- and electro-reduction of protons into H_2.[1] Nevertheless, they have been rarely placed within protein scaffolds and studied for their artificial hydrogenase activities.[24] To our knowledge, this was limited to the work by the groups of Hayashi and Ghirlanda. The former one has covalently attached $[(\mu\text{-}S)_2Fe_2(CO)]_6$ species to cytochrome c[11] and nitrobindin[13] as well as to an octapeptide derived from cytochrome c556.[14] Ghirlanda et al. used an

helical 19-mer peptide to which the same $[(\mu\text{-}S)_2Fe_2(CO)]_6$ species was attached.[15] It was shown that the resulting hybrid proteins catalyzed the photoreduction of H^+ into H_2, using ascorbate as a sacrificial electron donor and an inorganic photosensitizer for light absorption, in water, with initial TOF values ranging from 0.1 to 2 min^{-1}.

Here we used a series of [$2Fe^{HydA}$] mimics for preparing a novel class of artificial hydrogenases, which specifically contain a synthetic [6Fe] metallocofactor highly reminiscent of the H-cluster of HydA. For that purpose we chose the iron-sulfur HydF protein as the protein host and diiron complexes containing at least one cyanide ligand because we previously established that the CN^- ligand could coordinate one of the Fe atoms of the HydF [4Fe-4S] cluster, leading to a biomimetic [6Fe] cluster, exemplified in Figure 1B. This was previously established using complexes **1** and **2**.[16,22] We interpret the FTIR and EPR characteristics of the novel **4**-HydF hybrid, reported here, also in terms of the formation of a [6Fe] mimic of the H-cluster. That **4** is associated with the [4Fe-4S] cluster of HydF is also in line with the observation that mutations of glutamate 305, adjacent to the cluster, into cysteine or alanine had a large effect on the enzyme activity of **4**-HydF.

The approach, selecting HydF as the protein host rather than HydA, has the advantage that it might allow using a greater variety of [2Fe] complexes since HydA has been clearly shown to be designed, by natural evolution, for activating complex **1** almost exclusively.[23] We show here that not only HydF can bind a variety of analogs of **1** and **2**, in stoichiometric amounts, but also that some of the resulting hybrids display proton reduction activities, measured with the chemical dithionite/methyl viologen assay, classically used for the assessment of natural hydrogenases activity, greater than that of the **1**-HydF hybrid. It is interesting to note that these assay conditions, in contrast to photochemical assay conditions generally used for artificial hydrogenases, select catalytic systems working with very low overpotential requirements. Furthermore, our data show that HydF converts some of the tested synthetic mimics, inactive when free in aqueous solution, into active catalysts, within the hybrid, illustrating the potential of the artificial enzymology strategy.

Specifically, **4**-HydF, the analog of **2**-HydF with Se bridging atoms in place of S atoms, is, by far, the most active artificial hydrogenase and its activity compares well with artificial hydrogenases based on [2Fe] complexes reported by the groups of Hayashi and Ghirlanda discussed above. In particular, **4**-HydF is 13 times more active than **2**-

HydF and it is also much more stable during catalysis. As **5**-HydF, the analog of **1**-HydF with Se bridging atoms in place of S atoms, is also more active than **1**-HydF, these data obviously demonstrate a specific stimulating effect of Se vs S as bridging atoms. This finding is in line with previous observations on Se-incorporated diiron mimics revealing higher electrochemical hydrogen evolution activity and higher stability in aqueous solution.[21,25,26] It was indeed proposed that the replacement of μ-S atoms by Se atoms enhances the electron density and the basicity of the iron core, which makes it more susceptible to protonation. The increased density in the CN^- bridge might also contribute to the enhanced strength of the bond between **4** and the [4Fe-4S] cluster.

There are several intriguing observations that deserve some specific comments. First, not anticipated, hybrids **2**-HydF and **4**-HydF with a methylene bridgehead group are more active than the analogs, **1**-HydF and **5**-HydF, with an amine group and than **3**-HydF, with an oxygen bridgehead atom. This is highly surprising since it is a well-established dogma that the amine group is essential in HydA, for proton transfer. We even confirmed that **1**-HydF was totally inactive.[17] Since the amine function is lacking in the active HydF hybrids, this suggests that another proton shuttle should operate in order to explain their activities. Whether this function is carried out by the chalcogenide atoms or whether protonation occurs directly at the diiron center is difficult to conclude at this stage. Second, while it is likely that indeed proton reduction takes place at the diiron complex, as in HydA, we observed that the only reduced state that can be trapped and characterized spectroscopically has the extra electron localized on the [4Fe-4S] cluster. This opens the intriguing possibility of a different enzyme mechanism for HydF-based artificial hydrogenases, in which the [4Fe-4S] cluster would play a more important role in accumulating and using charges. Third, we report here for the first time a synthetic diiron complex, namely **4**, that is slightly more efficiently activated by the HydF protein host than by HydA (compare **4**-HydF and **4**-HydA activities), showing a unique case in which the [6Fe] cluster of HydF (Figure 1B) is more active than the [6Fe] cluster of HydA (Figure 1A). Thus, it is interesting to note that differential effects of the protein scaffold, HydF or HydA, were observed with respect to the activity of the diiron complex inserted in the protein. HydA has a dramatic stimulating effect on diiron complexes exclusively when the latter carry an amine group in the bridge: **2**-HydA and **4**-HydA display a

very poor activity as compared to **1**-HydA and **5**-HydA, as previously reported.[17,20,23] In contrast, the most active HydF hybrid is **4**-HydF, with a methylene as the bridgehead group. These differences, which must in part account for differences of the respective [6Fe] clusters, specifically the cysteine vs cyanide bridge, might better be understood at the molecular level with a three-dimensional structure of a HydF hybrid, that is not available yet.

While the artificial hydrogenase based on HydF with a synthetic [6Fe] cluster as the metallocofactor is far from comparing favorably with fully active HydA in terms of HER activity, the present work indicates that it forms a suitable platform towards the development of more efficient enzymes. Via the exploration of a large scope of synthetic [2Fe] complexes, in fact larger than in the case of HydA, and the appropriate mutations of amino acids in the active site, guided by a three-dimensional structure of the holo form, these artificial hydrogenases might evolve towards novel functional HydA-like enzymes. On the way, we might better understand how a polypeptide is able to activate a diiron complex. While a rational approach based on structure-directed mutagenesis might indeed improve the activity of such artificial hydrogenases, it is well established that optimization requires a combination of multiple mutations, including far away from the active site.[27] Thus, a random mutagenesis/directed evolution approach would even be more appropriate.[28] However, this requires very challenging screening anaerobic assays. The field of artificial hydrogenases will certainly go soon in this direction.

Experimental section

Overexpression and purification of apo-HydF

Apo-HydF was obtained as previously described.[17]

In vitro reconstitution of [4Fe-4S] cluster of apo-HydF

FeS-HydF was produced as previously described.[17]

In vitro reconstitution of [4Fe-4S] cluster of apo-HydF

Apo-HydF was incubated overnight with an excess of seleno-L-cystine, $Fe(SO_4)_2(NH_4)_2$ H_2O and DTT, in the presence of a catalytic amount of the *E.coli* cysteine desulfurase

CsdA under strictly anaerobic conditions in a MBraun glovebox with less than 0.5 ppm O_2. The excess of Fe(II) and seleno-L-cystine have been removed by size exclusion chromatography through a Superdex S200 10/300 GL column, equilibrated with 25 mM HEPES buffer pH 7.5, 200 mM NaCl, 5 mM DTT.

x-HydF hybrids preparation

FeS-HydF has been extensively washed with 25 mM HEPES buffer pH 7.5, 200 mM NaCl using Amicon Ultra 30 kDa centrifugation filters to remove any trace of DTT for preventing a decomposition of the organometallic complex and incubated for 1 h with 3-10 fold excess of the desired complex, previously dissolved in DMSO. The excess of it has been removed through desalting column (NAP-10; GE Healthcare).

1-7 synthesis

The synthetic complexes **1**-**7** have been synthesized as Et_4N^+ salts anaerobically according to previously reported procedures. [20,21,29–34] Compounds were dissolved in DMSO, stored in sealed vials and frozen at -80°C until use.

Fe quantitation

For each protein sample, the Fe content was determined in triplicate for two protein concentrations - according to the method of Fish.[35] In some cases Fe quantitation has been carried out with different protein preparations.

Hydrogen evolution activity assays

Hydrogen evolution activity was measured with a miniaturized Clark-type electrochemical H_2 microsensor (purchased from Unisense) polarized at +1000 mV. The hydrogen content was recorded at 1 s intervals with the SensorTrace software package by Unisense. The sensor has been calibrated in potassium phosphate pH 6.0 bubbled with 100% H_2.

The reaction mixture contained 4 µM **x**-HydF, 4 mM sodium dithionite, 100 mM potassium phosphate pH 6.0 and the reaction is started when 100 mM sodium dithionite is added to the solution. The assay is performed in a sealed "microrespiration" chamber to keep the solution anaerobic, unless differently stated.

Hydrogen evolution activity has been calculated as turnover frequency from the amount of H_2 formed after 5 min reaction.

Electron Paramagnetic Resonance spectroscopy

X-Band cw EPR spectra were recorded at T=14 K in a standard TE102 rectangular resonator on a Bruker Elexsys 500 spectrometer employing an Oxford ESR900 helium flow cryostat.

Fourier-Transform Infrared Spectroscopy

Transmission FTIR measurements were carried out with a Vertex 80v spectrometer from Bruker Optics using a liquid nitrogen cooled mercury cadmium telluride (MCT) detector. Samples were measured in CaF_2 cells without further treatment. Spectra were recorded at room temperature in forward-backward mode with a spectral resolution of 2 cm^{-1}. Data processing was performed by home written scripts in Matlab® programming environment.

Supporting information

Supplementary data for: UV-Vis spectra of hybrid proteins; hydrogen evolution activity of several hybrids, included those made with HydF mutants; FTIR spectra of **4**-HydF and its mutants; UV-Vis spectra during reduction of **4**-HydF and EPR parameters used for simulations of EPR spectra.

Acknowledgements

This work was supported by the French State Program 'Investissements d'Avenir' (Grants "LABEX DYNAMO", ANR-11-LABX-0011-01, "LABEX ARCANE", ANR-11-LABX-0003-01 and grant ANR-17-EURE-0003). F. W. thank for the financial support of the Deutsche Forschungsgemeinschaft, the Fraunhofer Internal Programs under Grant No. Attract 097-602175 and the Studienstiftung des deutschen Volkes.

References

(1) Lubitz, W.; Ogata, H.; Rüdiger, O.; Reijerse, E. Hydrogenases. *Chem. Rev.* **2014**, *114*, 4081–4148.

(2) Cracknell, J. A.; Vincent, K. A.; Armstrong, F. A. Enzymes as Working or Inspirational Electrocatalysts for Fuel Cells and Electrolysis. *Chem. Rev.* **2008**, *108*, 2439–2461.

(3) Simmons, T. R.; Berggren, G.; Bacchi, M.; Fontecave, M.; Artero, V. Mimicking Hydrogenases: From Biomimetics to Artificial Enzymes. *Coord. Chem. Rev.* **2014**, *270–271*, 127–150.

(4) Artero, V.; Chavarot-Kerlidou, M.; Fontecave, M. Splitting Water with Cobalt. *Angew. Chem. Int. Ed.* **2011**, *50*, 7238–7266.

(5) Artero, V.; Berggren, G.; Atta, M.; Caserta, G.; Roy, S.; Pecqueur, L.; Fontecave, M. From Enzyme Maturation to Synthetic Chemistry: The Case of Hydrogenases. *Acc. Chem. Res.* **2015**, *48*, 2380–2387.

(6) Ahmed, M. E. A.; Chattopadhyay, S. C.; Wang, L.; Brazzolotto, D.; Pramanik, D. P.; Aldakov, D. A.; Fize, J. F.; Morozan, A.; Gennari, M.; Duboc, C.; Abhishek, D.; Artero, V. Hydrogen Evolution from Aqueous Solution Mediated by a Heterogenized [NiFe]-Hydrogenase Model: Low PH Enables Catalysis through Enzyme-Relevant Mechanism. *Angew. Chem. Int. Ed.* **2018**, *57*, 16001-16004.

(7) Ginovska-Pangovska, B.; Dutta, A.; Reback, M. L.; Linehan, J. C.; Shaw, W. J. Beyond the Active Site: The Impact of the Outer Coordination Sphere on Electrocatalysts for Hydrogen Production and Oxidation. *Acc. Chem. Res.* **2014**, *47*, 2621–2630.

(8) Brezinski, W. P.; Karayilan, M.; Clary, K. E.; Pavlopoulos, N. G.; Li, S.; Fu, L.; Matyjaszewski, K.; Evans, D. H.; Glass, R. S.; Lichtenberger, D. L.; Pyun, J. [FeFe]-Hydrogenase Mimetic Metallopolymers with Enhanced Catalytic Activity for Hydrogen Production in Water. *Angew. Chem. Int. Ed.* **2018**, *57*, 11898–11902.

(9) Schwizer, F.; Okamoto, Y.; Heinisch, T.; Gu, Y.; Pellizzoni, M. M.; Lebrun, V.; Reuter, R.; Köhler, V.; Lewis, J. C.; Ward, T. R. Artificial Metalloenzymes: Reaction Scope and Optimization Strategies. *Chem. Rev.* **2018**, *118*, 142–231.

(10) Caserta, G.; Roy, S.; Atta, M.; Artero, V.; Fontecave, M. Artificial Hydrogenases: Biohybrid and Supramolecular Systems for Catalytic Hydrogen Production or Uptake. *Curr. Opin. Chem. Biol.* **2015**, *25*, 36–47.

(11) Sano, Y.; Onoda, A.; Hayashi, T. A Hydrogenase Model System Based on the Sequence of Cytochrome c: Photochemical Hydrogen Evolution in Aqueous Media. *Chem. Commun. Camb. Engl.* **2011**, *47*, 8229–8231.

(12) Wittkamp, F.; Senger, M.; Stripp, S. T.; Apfel, U.-P. [FeFe]-Hydrogenases: Recent Developments and Future Perspectives. *Chem. Commun.* **2018**, *54*, 5934–5942.

(13) Onoda, A.; Kihara, Y.; Fukumoto, K.; Sano, Y.; Hayashi, T. Photoinduced Hydrogen Evolution Catalyzed by a Synthetic Diiron Dithiolate Complex Embedded within a Protein Matrix. *ACS Catal.* **2014**, *4*, 2645–2648.

(14) Sano, Y.; Onoda, A.; Hayashi, T. Photocatalytic Hydrogen Evolution by a Diiron Hydrogenase Model Based on a Peptide Fragment of Cytochrome C556 with an Attached Diiron Carbonyl Cluster and an Attached Ruthenium Photosensitizer. *J. Inorg. Biochem.* **2012**, *108*, 159–162.

(15) Roy, A.; Madden, C.; Ghirlanda, G. Photo-Induced Hydrogen Production in a Helical Peptide Incorporating a [FeFe] Hydrogenase Active Site Mimic. *Chem. Commun. Camb. Engl.* **2012**, *48*, 9816–9818.

(16) Berggren, G.; Adamska, A.; Lambertz, C.; Simmons, T. R.; Esselborn, J.; Atta, M.; Gambarelli, S.; Mouesca, J.-M.; Reijerse, E.; Lubitz, W.; Happe, T.; Artero, V.;

Fontecave, F. Biomimetic Assembly and Activation of [FeFe]-Hydrogenases. *Nature* **2013**, *499*, 66–69.
(17) Caserta, G.; Pecqueur, L.; Adamska-Venkatesh, A.; Papini, C.; Roy, S.; Artero, V.; Atta, M.; Reijerse, E.; Lubitz, W.; Fontecave, M. Structural and Functional Characterization of the Hydrogenase-Maturation HydF Protein. *Nat. Chem. Biol.* **2017**, *13*, 779–784.
(18) Bortolus, M.; Costantini, P.; Doni, D.; Carbonera, D. Overview of the Maturation Machinery of the H-Cluster of [FeFe]-Hydrogenases with a Focus on HydF. *Int. J. Mol. Sci.* **2018**, *19*, 3118.
(19) Berggren, G.; Garcia-Serres, R.; Brazzolotto, X.; Clemancey, M.; Gambarelli, S.; Atta, M.; Latour, J.-M.; Hernández, H. L.; Subramanian, S.; Johnson, M. K.; Fontecave, F. An EPR/HYSCORE, Mössbauer, and Resonance Raman Study of the Hydrogenase Maturation Enzyme HydF: A Model for N-Coordination to [4Fe-4S] Clusters. *J. Biol. Inorg. Chem. JBIC Publ. Soc. Biol. Inorg. Chem.* **2014**, *19*, 75–84.
(20) Sommer, C.; Rumpel, S.; Roy, S.; Farès, C.; Artero, V.; Fontecave, M.; Reijerse, E.; Lubitz, W. Spectroscopic Investigations of a Semi-Synthetic [FeFe] Hydrogenase with Propane Di-Selenol as Bridging Ligand in the Binuclear Subsite: Comparison to the Wild Type and Propane Di-Thiol Variants. *JBIC J. Biol. Inorg. Chem.* **2018**, *23*, 481-491.
(21) Kertess, L.; Wittkamp, F.; Sommer, C.; Esselborn, J.; Rüdiger, O.; Reijerse, E.; Hofmann, E.; Lubitz, W.; Winkler, M.; Happe, T.; Apfel, U.-P. Chalcogenide Substitution in the [2Fe]-Cluster of [FeFe]-Hydrogenases Conserves High Enzymatic Activity. *Dalton Trans.* **2017**, *46*, 16947-16958.
(22) Esselborn, J.; Lambertz, C.; Adamska-Venkatesh, A.; Simmons, T.; Berggren, G.; Noth, J.; Siebel, J.; Hemschemeier, A.; Artero, V.; Reijerse, E.; Fontecave, M.; Lubitz, W.; Happe, T. Spontaneous Activation of [FeFe]-Hydrogenases by an Inorganic [2Fe] Active Site Mimic. *Nat. Chem. Biol.* **2013**, *9*, 607–609.
(23) Siebel, J. F.; Adamska-Venkatesh, A.; Weber, K.; Rumpel, S.; Reijerse, E.; Lubitz, W. Hybrid [FeFe]-Hydrogenases with Modified Active Sites Show Remarkable Residual Enzymatic Activity. *Biochemistry* **2015**, *54*, 1474–1483.
(24) Dürrenberger, M.; Ward, T. R. Recent Achievments in the Design and Engineering of Artificial Metalloenzymes. *Curr. Opin. Chem. Biol.* **2014**, *19*, 99–106.
(25) Harb, M. K.; Apfel, U.-P.; Sakamoto, T.; El-khateeb, M.; Weigand, W. Diiron Dichalcogenolato (Se and Te) Complexes: Models for the Active Site of [FeFe] Hydrogenase. *Eur. J. Inorg. Chem.* **2011**, *2011*, 986–993.
(26) Apfel, U.-P.; Halpin, Y.; Gottschaldt, M.; Görls, H.; Vos, J. G.; Weigand, W. Functionalized Sugars as Ligands towards Water-Soluble [Fe-Only] Hydrogenase Models. *Eur. J. Inorg. Chem.* **2008**, *2008*, 5112–5118.
(27) Arnold, F. H. Directed Evolution: Bringing New Chemistry to Life. Angew. Chem. Int. Ed. **2018**, *57*, 4143–4148.
(28) Markel, U.; Sauer, D. F.; Schiffels, J.; Okuda, J.; Schwaneberg, U. Towards the Evolution of Artificial Metalloenzymes-A Protein Engineer's Perspective. Angew. Chem. Int. Ed. **2019**, *58*, 4454–4464.
(29) Li, H.; Rauchfuss, T. B. Iron Carbonyl Sulfides, Formaldehyde, and Amines Condense to Give the Proposed Azadithiolate Cofactor of the Fe-Only Hydrogenases. *J. Am. Chem. Soc.* **2002**, *124*, 726–727.
(30) Fiedler, A. T.; Brunold, T. C. Combined Spectroscopic/Computational Study of Binuclear Fe(I)−Fe(I) Complexes: Implications for the Fully-Reduced Active-Site Cluster of Fe-Only Hydrogenases. *Inorg. Chem.* **2005**, *44*, 1794–1809.

(31) Song, L.-C.; Yang, Z.-Y.; Bian, H.-Z.; Hu, Q.-M. Novel Single and Double Diiron Oxadithiolates as Models for the Active Site of [Fe]-Only Hydrogenases. *Organometallics* **2004**, *23*, 3082–3084.
(32) Ott, S.; Borgström, M.; Kritikos, M.; Lomoth, R.; Bergquist, J.; Åkermark, B.; Hammarström, L.; Sun, L. Model of the Iron Hydrogenase Active Site Covalently Linked to a Ruthenium Photosensitizer: Synthesis and Photophysical Properties. *Inorg. Chem.* **2004**, *43*, 4683–4692.
(33) Gloaguen, F.; Lawrence, J. D.; Schmidt, M.; Wilson, S. R.; Rauchfuss, T. B. Synthetic and Structural Studies on $[Fe_2(SR)_2(CN)_x(CO)_{6-x}]^{(x-)}$ as Active Site Models for Fe-Only Hydrogenases. *J. Am. Chem. Soc.* **2001**, *123*, 12518–12527.
(34) Esmieu, C.; Berggren, G. Characterization of a Monocyanide Model of FeFe Hydrogenases – Highlighting the Importance of the Bridgehead Nitrogen for Catalysis. *Dalton Trans.* **2016**, *45*, 19242–19248.
(35) Fish, W. W. Rapid Colorimetric Micromethod for the Quantitation of Complexed Iron in Biological Samples. *Methods Enzymol.* **1988**, *158*, 357–364.

Figure.1: Schematic representation of (A) the active site (H-cluster) of [FeFe]-hydrogenases (HydA) and (B) the [6Fe] center of the artificial hydrogenase obtained by association of a [2Fe] synthetic complex **1** with the [4Fe-4S] cluster of HydF.

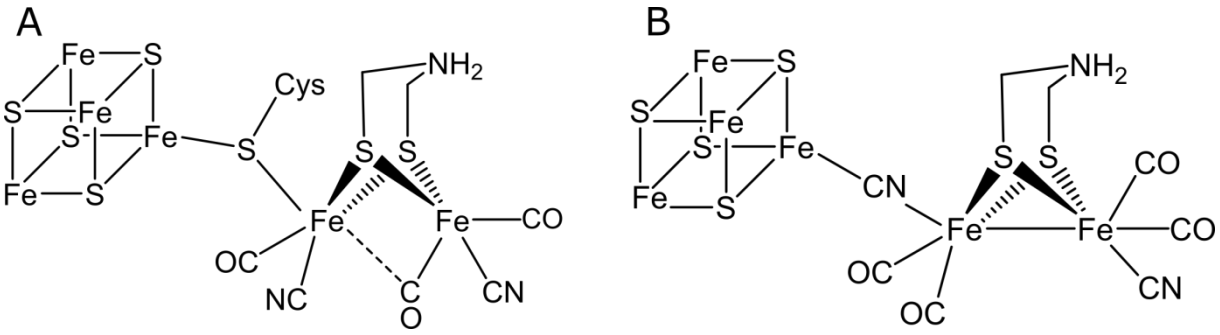

Scheme 1 : Synthetic diiron complexes used in this study.

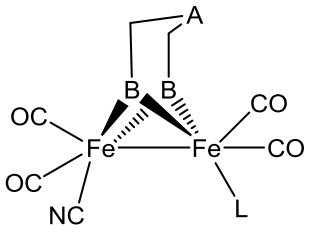

X	Formula of complex X	A	B	L
1	$[Fe_2(adt)(CO)_4(CN)_2]^{2-}$	NH	S	CN
2	$[Fe_2(pdt)(CO)_4(CN)_2]^{2-}$	CH_2	S	CN
3	$[Fe_2(odt)(CO)_4(CN)_2]^{2-}$	O	S	CN
4	$[Fe_2(pdSe)(CO)_4(CN)_2]^{2-}$	CH_2	Se	CN
5	$[Fe_2(adSe)(CO)_4(CN)_2]^{2-}$	NH	Se	CN
6	$[Fe_2(bp\text{-}adt)(CO)_4(CN)_2]^{2-}$	N-Ph-Br	S	CN
7	$[Fe_2(pdt)(CO)_5(CN)]^{-}$	CH_2	S	CO

adt^{2-}=azapropanedithiolate; pdt^{2-}=propanedithiolate; odt^{2-}=oxapropanedithiolate; $pdSe^{2-}$ =propanediselenolate; $adSe^{2-}$=azapropanediselenolate; $bp\text{-}adt^{2-}$=bromophenyl-azapropanedithiolate

Table 1: Fe content and TOF obtained for each hybrid protein.

Hybrid	2Fe content*	TOF** (min^{-1})
1-HydF	0.4 ± 0.0	/
2-HydF	0.8 ± 0.2	0.05 ± 0.01
3-HydF	0.4 ± 0.1	/
4-HydF	0.9 ± 0.2	0.65 ± 0.04
5-HydF	1.5 ± 0.2	0.12 ± 0.01
6-HydF	0.7 ± 0.2	0.10 ± 0.01
7-HydF	0.7 ± 0.1	0.07 ± 0.02
4-HydA	0.6 ± 0.2	0.24 ± 0.03
4-HydF E305C	0.8 ± 0.1	0.26 ± 0.02
4-HydF E305H	0.8 ± 0.2	0.65 ± 0.11
4-HydF E305A	0.7 ± 0.1	0.29 ± 0.03

*Fe content defined as the ratio of diiron complex to monomer of protein

TOF (Turnover Frequency) calculated from data collected over 5 min. The value for the control experiment using complex **4 in the absence of HydF is 0.08 min^{-1}

/ we consider as non-significant all the TOF values ≤ 0.02 min^{-1}

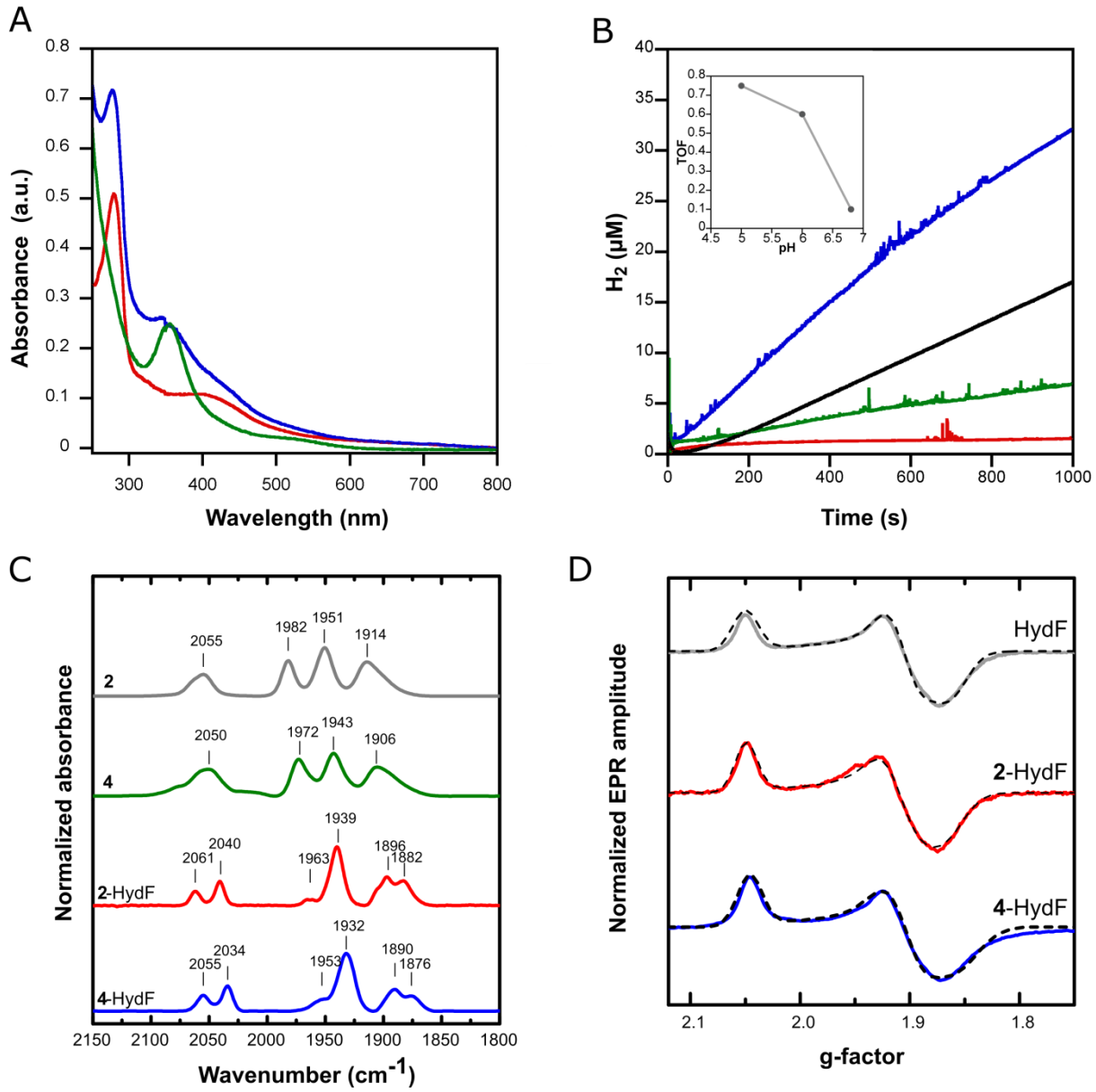

Figure 2: Characterization of 4-HydF

A) UV-Visible absorption spectra of 10 µM HydF (red), 10 µM **4**-HydF 10 µM (blue), 40 µM of **4** (green) in 25 mM HEPES buffer pH 7.5, 200 mM NaCl; B) Hydrogen evolution activity of 4 µM HydF (red), 4 µM **4**-HydA (black), 4 µM **4** (green) and 4 µM **4**-HydF (blue) in the presence of 4 mM sodium dithionite, 4 mM methyl viologen in phosphate buffer pH 6.0. The inset shows the TOF variability as function of pH; C) FTIR absorption spectra of **2**, **4**, as isolated **2**-HydF and as isolated **4**-HydF; D) X-band EPR spectra and simulations (dashed lines) of reduced HydF, reduced **2**-HydF and reduced **4**-HydF at T=14 K. The *g* values (g1/g2/g3) and g-strains are given in Table S1.